



ELSEVIER

Contents lists available at ScienceDirect

Bioorganic Chemistry

journal homepage: www.elsevier.com/locate/bioorg

Antibacterial activity against drug-resistant microbial pathogens of cytochalasan alkaloids from the arthropod-associated fungus *Chaetomium globosum* TW1-1

Weixi Gao^{a,1}, Yan He^{b,1}, Fengli Li^a, Chenwei Chai^a, Jinwen Zhang^b, Jieru Guo^b, Chunmei Chen^a, Jianping Wang^a, Hucheng Zhu^a, Zhengxi Hu^{a,*}, Yonghui Zhang^{a,*}

^a Hubei Key Laboratory of Natural Medicinal Chemistry and Resource Evaluation, School of Pharmacy, Tongji Medical College, Huazhong University of Science and Technology, Wuhan 430030, People's Republic of China

^b Tongji Hospital, Tongji Medical College, Huazhong University of Science and Technology, Wuhan 430030, People's Republic of China

ARTICLE INFO

InChIKey:

XGACFKGMUHQKPG-UDAZEODHSA-

NKeywords:

Chaetomium globosum TW1-1

Feeding experiment

Cytochalasan alkaloids

Antibacterial activity

ABSTRACT

By feeding 1-methyl-L-tryptophan (1-MT) into cultures of the arthropod-associated fungus *Chaetomium globosum* TW1-1, three novel cytochalasan alkaloids, termed as armochaetoglosins A–C (1–3), together with five known analogues, namely prochaetoglobosin I (4), chaetoglobosin T (5), chaetoglobosin C (6), armochaetoglobosin Y (7), and chaetoglobosin V₁ (8), were isolated and characterized. Their structures including absolute configurations were elucidated by means of NMR spectroscopy, single-crystal X-ray crystallography, and comparison of the experimental electronic circular dichroism (ECD) spectra. Structurally, compounds 1–3 represented the first examples of 1'-N-methyl-chaetoglobosins, which were possibly biosynthesized from the additive 1-MT rather than tryptophan. Additionally, compound 3 showed the highest antibacterial activity against *K. pneumoniae* and ESBL-*E. coli* with MIC values of 4.0 μg/mL and 16.0 μg/mL, respectively, wherein the inhibitory effect of 3 against *K. pneumoniae* was stronger than that of the clinically used antibiotic meropenem, with an MIC value of 8 μg/mL. Our findings may provide new chemical templates for the development of new antibacterial agents against drug-resistant microbial pathogens.

1. Introduction

The rise of antibiotic-resistant bacteria is a severe health care problem worldwide [1]. In particular, methicillin-resistant *Staphylococcus aureus* (MRSA) and ESBL-producing and carbapenemase-producing Gram-negative bacteria such as *Escherichia coli*, *Pseudomonas aeruginosa*, and *Klebsiella pneumoniae* have risen at an alarming pace, which challenged clinicians in the treatment of antimicrobial-resistant infections, including the major surgery, transplant operations, and biomedical device-related infections [2]. Therefore, the discovery of novel antibacterial natural products with new mechanisms of action is urgent to resolve the antibiotic resistance crisis.

Cytochalasan alkaloids represent a large group of fungal metabolites with potential bioactivities, such as antitumor [3], nematocidal [4], immunomodulatory [5], and antibacterial [6] activities. Previously,

Tan and co-workers have found that a silent fungal Pictet–Spenglerase (FPS) gene of *Chaetomium globosum* 1C51 could be activable by 1-methyl-L-tryptophan (1-MT), thus enabling the Pictet–Spengler reaction between 1-MT and flavipin to create skeletally unprecedented compounds [7]. Inspired by this peculiar idea and aimed at discovering novel cytochalasan alkaloids as antibacterial agents against drug-resistant microbial pathogens from a genetically powerful and cytochalasan-producing fungus *Chaetomium globosum* TW1-1, which was isolated from the medicinal terrestrial arthropod *Armadillidium vulgare* [8,9], the 1-methyl-L-tryptophan (1-MT) was fed into the fermented rice substrate of this strain to activate its silent genes to maximize cytochalasan alkaloid diversity, which resulted in the isolation of three novel cytochalasan alkaloids (1–3) and five known analogues (4–8). In this study, we report the isolation, structure elucidation, and bioactivity evaluation of these compounds (Fig. 1).

* Corresponding authors.

E-mail addresses: hzx616@126.com (Z. Hu), zhangyh@mails.tjmu.edu.cn (Y. Zhang).

¹ These authors contributed equally to this work.

<https://doi.org/10.1016/j.bioorg.2018.10.020>

Received 6 September 2018; Received in revised form 5 October 2018; Accepted 9 October 2018

Available online 10 October 2018

0045-2068/ © 2018 Elsevier Inc. All rights reserved.

Table 1
¹H NMR spectroscopic data (δ in ppm, J in Hz) for compounds 1–3.

No.	1 ^{a,b}	2 ^{c,d}	3 ^{a,d}
4	2.72, dd (5.7, 2.7)	2.42, dd (15.2, 10.0)	2.71, dd (6.2, 1.7)
5	2.41, m	2.30, m	1.70, m
7	5.34, br. s	5.42, br. s	2.89, d (6.1)
8	2.78, m	2.52, m	2.31, dd (10.5, 6.0)
10	2.78, m; 2.42, m	2.84, dd (14.5, 3.8); 2.57, dd (14.5, 3.6)	2.85, m; 2.65, m
11	1.04, d (7.2)	1.19, d (7.2)	0.88, d (7.3)
12	1.73, s	3.94, s	1.22, s
13	5.94, ddd (15.3, 9.7, 1.9)	5.87, dd (15.3, 10.0)	6.34, dd (15.5, 10.5)
14	5.05, ddd (15.3, 10.3, 3.2)	4.82, ddd (15.3, 11.2, 5.5)	5.24, ddd (15.5, 11.8, 2.7)
15	2.19, m; 1.78, m	2.06, m; 1.67, m	2.61, m; 1.81, m
16	2.42, m	2.21, m	2.34, m
17	4.96, dd (9.4, 1.6)	4.76, br. d (8.3)	2.81, d (4.5)
19	4.10, dd (9.2, 6.2)	1.90, m; 1.66, m	5.90, m
20	2.35, m	1.67, m; 1.45, m	
21	6.41, ddd (15.7, 7.9, 6.1)	0.62, m	2.54, t (6.6)
22	6.22, dd (15.7, 1.4)	2.68, ddd (19.3, 11.6, 3.0); 0.93, ddd (19.3, 11.7, 4.8)	2.93, d (5.6); 1.57, dd (14.3, 7.9)
24	0.94, d (6.7)	0.83, d (6.7)	0.66, d (6.8)
25	1.52, s	1.37, s	2.08, s
2'	6.89, s	7.02, s	6.91, s
3'			
4'	7.49, d (7.8)	7.54, d (7.9)	7.46, d (7.8)
5'	7.02, m	7.00, m	7.04, m
6'	7.13, m	7.09, m	7.13, m
7'	7.27, d (8.0)	7.28, d (8.1)	7.25, d (8.2)
8'	3.71 s	3.68, s	3.71, s

^a In methanol-*d*₄.^b Recorded at 600 MHz.^c In DMSO-*d*₆.^d Recorded at 400 MHz.

2.5. Spectroscopic data of compounds

Armochaetoglosin A (1): C₃₃H₄₀N₂O₃; colorless needle crystals; $[\alpha]_D^{20}$: -82 (c 0.1, MeOH); UV (MeOH) λ_{\max} (log ϵ) 202 (4.79), 224 (4.70), 284 (3.80) nm; IR ν_{\max} 3433, 2960, 2923, 1681, 1619, 1455, 1434, 1381, 1327, 1303, 1160, 1034, 1015, 970, 740 cm⁻¹; ECD (MeOH) λ_{\max} ($\Delta\epsilon$) 220 (-25.4) nm; For ¹H NMR (600 MHz) and ¹³C NMR (150 MHz) data, see Tables 1 and 2; HRESIMS m/z 513.3101 [M+H]⁺ (calcd for C₃₃H₄₁N₂O₃, 513.3117) and m/z 535.2935 [M+Na]⁺ (calcd for C₃₃H₄₀N₂O₃Na, 535.2937).

Armochaetoglosin B (2): C₃₃H₄₂N₂O₃; white powders; $[\alpha]_D^{20}$: -51 (c 0.1, MeOH); UV (MeOH) λ_{\max} (log ϵ) 202 (4.39), 224 (4.25), 289 (3.54) nm; IR ν_{\max} 3430, 2932, 2859, 1632, 1451, 1382, 1029, 740, 596 cm⁻¹; ECD (MeOH) λ_{\max} ($\Delta\epsilon$) 224 (-16.8) nm; For ¹H NMR (400 MHz) and ¹³C NMR (100 MHz) data, see Tables 1 and 2; HRESIMS m/z 515.3275 [M+H]⁺ (calcd for C₃₃H₄₃N₂O₃, 515.3274) and m/z 537.3041 [M+Na]⁺ (calcd for C₃₃H₄₂N₂O₃Na, 537.3093).

Armochaetoglosin C (3): C₃₃H₃₈N₂O₄; white powders; $[\alpha]_D^{20}$: +18 (c 0.1, MeOH); UV (MeOH) λ_{\max} (log ϵ) 205 (4.42), 223 (4.47), 286 (3.66), 362 (3.40) nm; IR ν_{\max} 3427, 2924, 2857, 1691, 1624, 1446, 1383, 1323, 1257, 1172, 1110, 1029, 744, 564 cm⁻¹; ECD (MeOH) λ_{\max} ($\Delta\epsilon$) 223 (+11.8) nm; For ¹H NMR (400 MHz) and ¹³C NMR (100 MHz) data, see Tables 1 and 2; HRESIMS m/z 549.2717 [M+Na]⁺ (calcd for C₃₃H₃₈N₂O₄Na, 549.2729).

2.6. X-ray crystal structure analysis

Crystals of compound 1 were obtained in MeOH with four drops of CH₂Cl₂ and two drops of water. Intensity data were acquired at 296 K on a Bruker APEX DUO diffractometer equipped with an APEX-II CCD using Cu K α radiation. Cell refinement and data reduction were

Table 2
¹³C NMR spectroscopic data (δ in ppm) for compounds 1–3.

No.	1 ^{a,b}	2 ^{c,d}	3 ^{a,d}
1	176.9, C	173.7, C	176.9, C
3	55.5, CH	53.0, CH	54.0, CH
4	51.0, CH	49.5, CH	49.6, CH
5	36.1, CH	34.2, CH	38.1, CH
6	140.7, C	142.8, C	58.8, C
7	127.4, CH	125.5, CH	62.2, CH
8	47.7, CH	47.2, CH	51.5, CH
9	68.4, C	66.3, C	68.2, C
10	33.6, CH ₂	31.3, CH ₂	33.7, CH ₂
11	13.8, CH ₃	12.6, CH ₃	12.9, CH ₃
12	19.9, CH ₃	61.6, CH ₂	19.6, CH ₃
13	130.7, CH	131.0, CH	131.4, CH
14	133.5, CH	129.9, CH	133.5, CH
15	41.9, CH ₂	41.7, CH ₂	39.6, CH ₂
16	33.3, CH	31.0, CH	32.4, CH
17	136.0, CH	133.1, CH	49.9, CH
18	134.8, C	130.8, C	183.6, C
19	78.4, CH	35.6, CH ₂	129.3, CH
20	37.1, CH ₂	21.0, CH ₂	212.2, C
21	143.5, CH	18.1, CH ₂	44.7, CH
22	129.8, CH	37.7, CH ₂	43.1, CH ₂
23	201.0, C	211.1, C	211.3, C
24	21.7, CH ₃	21.7, CH ₃	16.4, CH ₃
25	10.4, CH ₃	13.9, CH ₃	17.7, CH ₃
2'	129.6, CH	129.5, CH	129.8, CH
3'	110.0, C	108.0, C	109.5, C
4'	119.8, CH	119.2, CH	119.5, CH
5'	119.9, CH	118.6, CH	120.2, CH
6'	123.4, CH	120.9, CH	122.6, CH
7'	110.1, CH	109.2, CH	110.2, CH
8'	32.7, CH ₃	32.2, CH ₃	32.7, CH ₃
1'a	138.6, C	128.4, C	138.5, C
3'a	129.7, C	128.4, C	129.4, C

^a In methanol-*d*₄.^b Recorded at 150 MHz.^c In DMSO-*d*₆.^d Recorded at 100 MHz.

performed by Bruker SAINT. The structure was solved by direct methods with SHELXL-2014/7. Refinements were performed with SHELXL-2014/7 using full-matrix least-squares, with anisotropic displacement parameters used for all the non-hydrogen atoms. The hydrogen atoms were located in the calculated positions and refined with a riding model. Molecular graphic was computed with PLATON. The crystallographic data for 1 (deposition No. CCDC 1835470) have been deposited in the Cambridge Crystallographic Data Centre. Copies of the data can be obtained free of charge on application to CCDC, 12 Union Road, Cambridge CB 1EZ, UK [fax: Int. +44 (0) (1223) 336 033; e-mail: deposi@ccdc.cam.ac.uk].

Crystallographic data for compound 1: C₃₃H₄₀N₂O₃, $M = 512.67$, orthorhombic, $a = 10.413(3)$ Å, $b = 13.900(4)$ Å, $c = 19.553(5)$ Å, $\alpha = 90.00^\circ$, $\beta = 90.00^\circ$, $\gamma = 90.00^\circ$, $V = 2830.2(13)$ Å³, $T = 296(2)$ K, space group $P2_12_12_1$, $Z = 4$, $\mu(\text{Cu K}\alpha) = 0.601$ mm⁻¹, 10557 reflections measured, 3937 independent reflections ($R_{\text{int}} = 0.1666$). The final R_1 values were 0.0655 ($I > 2\sigma(I)$). The final $wR(F^2)$ values were 0.1440 ($I > 2\sigma(I)$). The final R_1 values were 0.1732 (all data). The final $wR(F^2)$ values were 0.1941 (all data). The goodness of fit on F^2 was 0.980. Flack parameter = -0.3(4).

2.7. Biological assay protocols

2.7.1. Strains, media, and antibiotics

The test strains were obtained from the ATCC: methicillin-resistant *Staphylococcus aureus* ATCC 43300; *Enterococcus faecalis* ATCC 29212; ESBL-producing *Escherichia coli* ATCC 35218; *Pseudomonas aeruginosa* ATCC 15542; NDM-1-producing *Klebsiella pneumoniae* ATCC BAA2146. The reference compounds for the tests were recommended by the

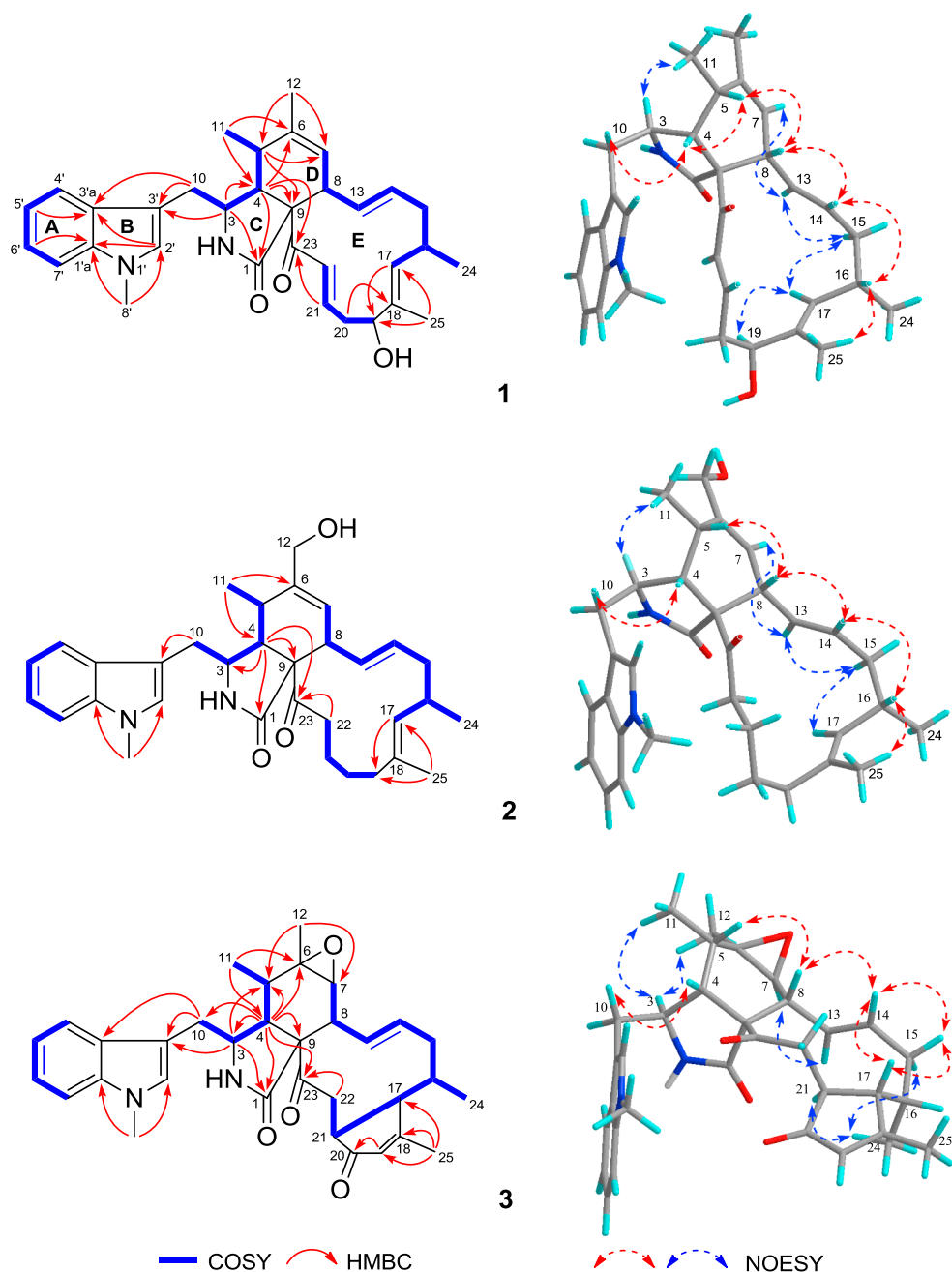


Fig. 2. Selected 2D NMR correlations of compounds 1–3.

National Committee for Clinical Laboratory Standards [10]: vancomycin (Sigma, cat # 861987); chloramphenicol (Sigma, cat # 1107300); amikacin (Sigma, cat # 1019508); ceftriaxone (Sigma, cat # 1098184); meropenem (Sigma, cat # M2574). All the investigated compounds 1–8 were $\geq 95\%$ pure (HPLC, wavelength = 210 nm). All compounds were dissolved in DMSO as 20 mg/mL stock solutions.

2.7.2. Determination of the minimum inhibitory concentrations (MICs)

Determination of the MICs were performed according to the previously reported broth microdilution method [11,12]. Briefly, the inoculum was standardized to almost 5×10^5 CFU/mL. Then, the plates were incubated at 37 °C for 16 h, and the MIC values were recorded as the lowest concentration of antibiotic, at which no visible bacterial growths were observed. Each experiment was carried out for three times.

2.7.3. Transmission electron microscope (TEM)

Transmission electron microscopy was used to confirm morphological changes after peptide exposure, according to the previously described method [13]. *K. pneumoniae* ATCC BAA2146 (10^8 CFU/mL) was exposed to MIC compound 3 (4 mg/mL) or $5 \times$ MIC compound 3 (20 mg/mL) for 2 h. After incubation at 37 °C, the bacteria were centrifuged at 10000 rpm for 10 min, washed twice with PBS (pH 7.4), and then prefixed in 2.5% glutaraldehyde in 0.2 M phosphate buffer (pH 7.3) to cross-link the proteins to preserve the morphological structure of the cells. The specimens were rinsed twice with the same buffer and post-fixed in 1% osmium tetroxide for 2 h, followed by a bloc staining with 2.0% uranyl acetate and dehydration in an ethanol series. The samples were then embedded in LR White resin (Sigma-Aldrich Co., Ltd, Shanghai, China), which was polymerized for 24 h at 60 °C. Embedded samples were thinly sectioned and stained by uranyl acetate and lead citrate before examination under a Tecnai G2 Spirit Twin electron

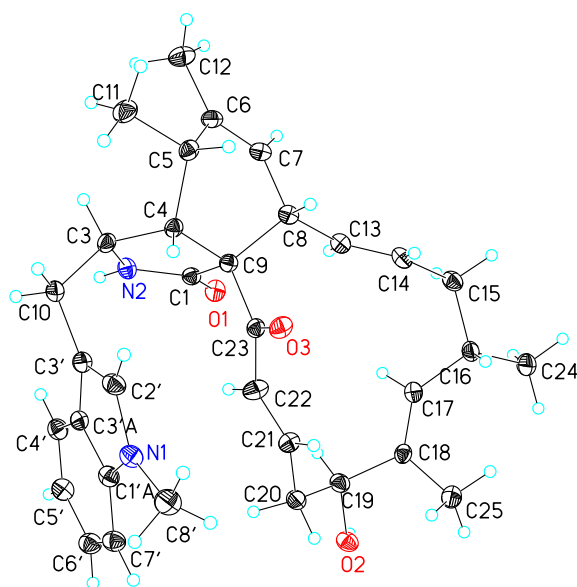


Fig. 3. ORTEP drawing of compound 1.

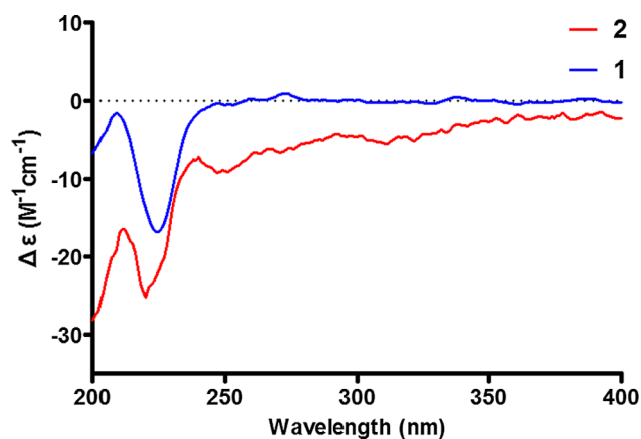


Fig. 4. Experimental ECD spectra of compounds 1 and 2 in MeOH.

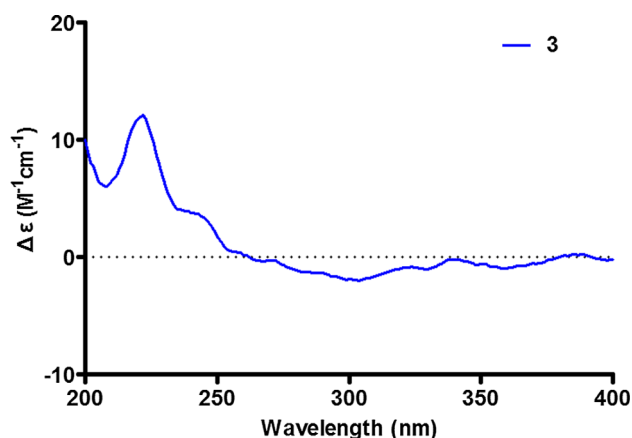


Fig. 5. Experimental ECD spectrum of compound 3 in MeOH.

microscope (FEI, USA). Experiments were repeated at least three times with different samples for bacteria.

2.7.4. Statistical analysis

Statistical analysis of the data was conducted using Graph Pad Prism 4.0 software. The collected data were expressed as the means \pm SD.

Values were analyzed using SPSS version 12.0 software via one-way analysis of variance (ANOVA), and $p < 0.05$ was considered statistically significant.

3. Results and discussion

3.1. Structural elucidations of armochaetoglosins A–C (1–3)

Compound 1 was obtained as colorless crystals with $[\alpha]_D^{20} -82$ (c 0.1, MeOH). Its molecular formula, $C_{33}H_{40}N_2O_3$, was deduced from the HRESIMS (m/z 535.2935 $[M+Na]^+$, calcd for $C_{33}H_{40}N_2O_3Na$, 535.2937) and ^{13}C NMR data, requiring 15 degrees of unsaturation. The IR absorptions of 1 implied the presence of amino (3433 cm^{-1}), carbonyl (1681 cm^{-1}), and double bond (1619 and 1455 cm^{-1}) functionalities. Analysis of its 1H , ^{13}C and DEPT NMR data (Tables 1 and 2) revealed 33 carbons, including five methyl groups [two secondary ones (δ_H 0.94/ δ_C 21.7; δ_H 1.04/ δ_C 13.8), two singlet ones (δ_H 1.52/ δ_C 10.4; δ_H 1.73/ δ_C 19.9), and one *N*-methyl (δ_H 3.71/ δ_C 32.7)], three sp^3 methylenes, seventeen methines [one oxymethine (δ_C 78.4) and eleven olefinic carbons], and eight quaternary carbons [one amide carbonyl (δ_C 176.9), one keto carbonyl (δ_C 201.0), and five olefinic carbons]. These carbon assignments along with two nitrogen atoms in the molecular formula suggested that compound 1 was most likely to be a chaetoglobosin-based alkaloid.

Detailed examination of the 1H - 1H COSY and HMBC spectra for 1 led to identification of the partial structural units as shown in Fig. 2. The 3'-substituted 1'-*N*-methyl-indolyl group (A and B rings) was elucidated based on the 1H - 1H COSY cross-peaks of H-4'/H-5'/H-6'/H-7' and HMBC correlations of H-2' with C-1'a and C-3'a, of H-5' with C-3'a, of H-6' with C-1'a, and of H₃-8' with C-1'a and C-2' (Fig. 2). Moreover, a key 1H - 1H COSY correlation of H-3/H-4 and the main HMBC correlations of H-3 and H-4 with the amide carbonyl C-1 and of H-4 with C-9 indicated the presence of a pyrrolidine-2-one moiety (C ring). Connectivity from the 1'-*N*-methyl-indolyl group (A and B rings) to the pyrrolidine-2-one unit (C ring) through the "C-3'-CH₂-10-CH-3" fragment was elucidated based on the key 1H - 1H COSY correlation of H-3/H₂-10 and long-range HMBC correlations of H-3 and H₂-10 with C-3'.

Furthermore, the cyclohexane ring (D ring) with two methyl groups attached at C-5 and C-6 and a $\Delta^{6,7}$ double bond, was established by the 1H - 1H COSY cross-peaks (Fig. 2) of H-4/H-5/H₃-11 and H-7/H-8 and the HMBC correlations (Fig. 2) of H-4 with C-6 and C-9, of H-5 with C-7 and C-9, of H₃-11 with C-4 and C-6, and of H₃-12 with C-5 and C-7. The 13-membered macrocyclic ring (E ring) with two methyl groups group at C-16 and C-18, a hydroxyl group at C-19, a keto carbonyl group at C-23, and three double bonds ($\Delta^{13,14}$, $\Delta^{17,18}$, and $\Delta^{21,22}$), was established based on the 1H - 1H COSY cross-peaks (Fig. 2) of H-8/H-13/H-14/H₂-15/H-16(H-16/H₃-24)/H-17 and H-19/H₂-20/H-21/H-22 and HMBC correlations (Fig. 2) of H-4 and H-21 with C-23 and of H₃-25 with C-17 and C-19. Accordingly, the planar structure of 1 was defined.

In the NOESY spectrum (Fig. 2), the NOE correlation between H-5 and H-8 β and the lacking NOE correlation of H-4/H-8 β suggested that the cyclohexane ring (D ring) was in a boat conformation with the β -orientations for H-5 and H-8, in consistent with previous reported chaetoglobosins [6]. The NOE correlations of H-3/H₃-11, H-4/H-10 β (δ_H 2.42), and H-4/H-5 suggested that H-4 was β -oriented, while H-3 was α -oriented. Furthermore, key NOE cross-peaks of H-8/H-14/H-16 suggested that H-8 and H-16 were cofacial and β -oriented. The observation of NOE cross-peaks of H-13/H-15 α (δ_H 1.78)/H-17/H-19 suggested that H-19 should be α -oriented. Moreover, the *E*-geometries of $\Delta^{13,14}$, $\Delta^{21,22}$, and $\Delta^{17,18}$ double bonds were judged by the large coupling constants of $J^{13,14}$ (15.3 Hz) and $J^{21,22}$ (15.7 Hz) and the NOESY correlation of H-16/H₃-25, respectively. Thus, the relative stereochemistry of 1 was ascertained.

After repeated recrystallization with various two-phase or three-phase solvents, a suitable crystal of 1 was obtained and then subjected to single-crystal X-ray diffraction analysis with Cu K α (Fig. 3).

Table 3
Antibacterial activity of compounds 1–8 (MIC, $\mu\text{g/mL}$).

Pathogens	1	2	3	4	5	6	7	8	Reference ^f
MRSA ^a	64	> 128	32	> 128	> 128	> 128	32	> 128	0.5 (Va)
<i>E. faecalis</i> ^b	> 128	> 128	32	> 128	> 128	> 128	64	64	16 (Ch)
ESBL- <i>E. coli</i> ^c	32	32	16	64	64	> 128	32	64	2 (Am)
<i>P. aeruginosa</i> ^d	> 128	> 128	> 128	> 128	> 128	> 128	> 128	> 128	1 (Ce)
<i>K. pneumoniae</i> ^e	> 128	64	4	32	> 128	> 128	16	64	8 (Me)

^a MRSA = methicillin-resistant *Staphylococcus aureus* ATCC 43300.

^b *E. faecalis* = *Enterococcus faecalis* ATCC 29212.

^c ESBL-*E. coli* = ESBL-producing *Escherichia coli* ATCC 35218.

^d *P. aeruginosa* = *Pseudomonas aeruginosa* ATCC 15542.

^e *K. pneumoniae* = *Klebsiella pneumoniae* ATCC BAA2146.

^f The activity of reference compounds was recommended by the National Committee for Clinical Laboratory Standards (CLSI); Va = Vancomycin; Ch = Chloramphenicol; Am = Amikacin; Ce = Ceftriaxone; Me = Meropenem.

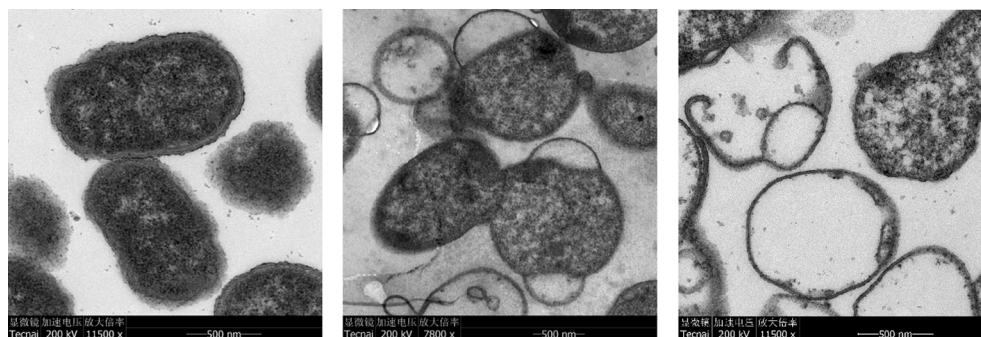


Fig. 6. TEM micrographs of *K. pneumoniae* ATCC BAA2146 incubated in LB broth (control), 4 mg/mL (MIC) and 20 mg/mL (5 × MIC) compound 3 at 37 °C for 2 h.

Unluckily, the refined Flack parameter [−0.30 (4)] only enabled us to define its relative stereochemistry as 3S*, 4R*, 5S*, 8S*, 9S*, 16S*, 19S*. Furthermore, by comparison of the ECD spectrum of 1 with that of previously reported armochaetoglobins H [8], the identical ECD curves suggested the absolute stereochemistry of 1 to be 3S, 4R, 5S, 8S, 9S, 16S, 19S. Therefore, the structure of 1 was defined and named armochaetoglosin A.

Compound 2 was obtained as a white powder. On the basis of the HRESIMS ion peaks at m/z 537.3041 $[\text{M} + \text{Na}]^+$ and m/z 515.3275 $[\text{M} + \text{H}]^+$ and ^{13}C NMR data, the molecular formula of 2 was elucidated as $\text{C}_{33}\text{H}_{42}\text{N}_2\text{O}_3$ with 14 degrees of unsaturation. A side-by-side comparison of the NMR data (Tables 1 and 2) of 2 with those of 1 suggested that compound 2 was structurally related to 1, with the differences being explained as follows: the replacement of a pair of olefinic carbons (δ_{C} 143.5, C-21; δ_{C} 129.8, C-22) by two aliphatic methylene carbons (δ_{C} 18.1, C-21; δ_{C} 37.7, C-22); one methyl carbon (δ_{C} 19.9, C-12) by an oxygenated methylene carbon (δ_{C} 61.6, C-12); and an oxygenated methine carbon (δ_{C} 78.4, C-19) by a methylene carbon (δ_{C} 35.6, C-19). These conclusions could be further confirmed by the ^1H – ^1H COSY spin system of H₂-19/H₂-20/H₂-21/H₂-22 and HMBC correlations (Fig. 2) of H-22 with C-23 and of H-17 and H₃-25 with C-19. The relative configuration of 2 was identical to that of 1, as supported by their similar NOESY spectra (Fig. 2). In addition, the measured ECD spectrum of 2 was almost identical to that of 1 (Fig. 4), indicating the same chiral centers for these two compounds. Therefore, the structure of 2 was defined and named armochaetoglosin B.

Compound 3 was isolated as a white powder, and the molecular formula $\text{C}_{33}\text{H}_{38}\text{N}_2\text{O}_4$ was determined based on the HRESIMS analysis (m/z 549.2717 $[\text{M} + \text{Na}]^+$). Interpretation of the ^1H and ^{13}C NMR data of 3 revealed that its structure was quite similar to that of armochaetoglobins Y (7) [14], with the only difference being that an additional *N*-methyl signal at δ_{C} 32.7 existed in 3, as supported by the HMBC correlations of H₃-8' with C-1'a and C-2'. The similar NOESY data (Fig. 2)

and experimental ECD spectra (Fig. 5) of 3 and armochaetoglobins Y [14] suggested that both compounds shared the same relative and absolute configurations. Therefore, the structure of 3 was defined and named armochaetoglosin C.

Five already known cytochalasan alkaloids were identified as prochaetoglobosin I (4) [15], chaetoglobosin T (5) [6], chaetoglobosin C (6) [16], armochaetoglobins Y (7) [14], and chaetoglobosin V_b (8) [17] by comparison of their NMR and HRESIMS data with the literature.

3.2. *In vitro* antibacterial activity against drug-resistant microbial pathogens

Compounds 1–8 were evaluated for antibacterial activity against five drug-resistant microbial pathogens, including methicillin-resistant *Staphylococcus aureus* (MRSA), *Enterococcus faecalis*; ESBL-producing *Escherichia coli*, *Pseudomonas aeruginosa*, and NDM-1-producing *Klebsiella pneumoniae*. Highest antibacterial activity against NDM-1-producing *K. pneumoniae* and ESBL-producing *E. coli* for compound 3 were observed (Table 3), with MIC values of 4.0 $\mu\text{g/mL}$ and 16.0 $\mu\text{g/mL}$, respectively, wherein the inhibitory effect of 3 against NDM-1-producing *K. pneumoniae* was stronger than that of the clinically used antibiotic meropenem, with an MIC value of 8 $\mu\text{g/mL}$. To directly visualize the effect of 3 on the bacterial membrane, the transmission electron microscopy was applied to examine the morphological changes in *K. pneumoniae* after treatment with 4 mg/mL and 20 mg/mL compound 3 for 2 h. In contrast to the smooth, continuous membrane structure clearly visible in untreated bacteria, the cytoplasmic membrane of compound 3 treated cells was almost completely disrupted, and some cellular contents had leaked out (Fig. 6). Moreover, comparison of the antibacterial activity of 1/5 and 3/7 suggested that 1'-*N*-methylation could enhance the inhibitory potency against several drug-resistant microbial pathogens, and this might provide useful reference for the design and exploitation of new antibacterial agents.

4. Conclusions

By feeding 1-methyl-L-tryptophan (1-MT) into cultures of the fungus *Chaetomium globosum* TW1-1 to activate silent genes to maximize cytochalasan alkaloid diversity, three novel cytochalasan alkaloids, termed as armochaetoglosins A–C (1–3), together with five known analogues (4–8), were isolated and characterized. Structurally, compounds 1–3 represented the first examples of 1'-N-methyl-chaetoglobosins, which were possibly biosynthesized from the additive 1-MT rather than tryptophan. In the antibacterial assay, compound 3 showed the highest antibacterial activity against NDM-1-producing *K. pneumoniae* and ESBL-producing *E. coli* with MIC values of 4.0 µg/mL and 16.0 µg/mL, respectively, wherein the inhibitory effect of 3 against NDM-1-producing *K. pneumoniae* was stronger than that of the clinically used antibiotic meropenem, with an MIC value of 8 µg/mL. Under the severe situation that antibiotic resistance is a growing public threat, our prominent findings may help to understand the mechanisms of bacterial resistance and provide new chemical templates for the development of new antibacterial agents against drug-resistant microbial pathogens.

5. Notes

The authors declare no competing financial interest.

Acknowledgments

We thank the Analytical and Testing Center at Huazhong University of Science and Technology for measuring ECD and IR spectra. In addition, we would like to thank Pei Zhang and An-Na Du from the Core Facility and Technical Support, Wuhan Institute of Virology for their help to produce TEM micrographs. This work was financially supported by the Program for Changjiang Scholars of Ministry of Education of the People's Republic of China (No. T2016088), the National Natural Science Foundation for Distinguished Young Scholars (No. 81725021), the Innovative Research Groups of the National Natural Science Foundation of China (No. 81721005), the China Postdoctoral Science Foundation Funded Project (Nos. 2017M610479 and 2018T110777), the National Natural Science Foundation of China (Nos. 81573316,

21702067, and 81803387), and the Hubei Provincial Natural Science Foundation of China (No. 2018CFB152).

Appendix A. Supplementary material

Supplementary data to this article can be found online at <https://doi.org/10.1016/j.bioorg.2018.10.020>. These data include MOL files and InChIKeys of the most important compounds described in this article.

References

- [1] Centers for Disease Control, Antibiotic resistance threats in the United States CDC, Atlanta, 2013.
- [2] D.W. Gerard, *Nat. Prod. Rep.* 34 (2017) 694–701.
- [3] D. Zhang, H. Ge, D. Xie, R. Chen, J.H. Zou, X. Tao, J. Dai, *Org. Lett.* 15 (2013) 1674–1677.
- [4] Y. Hu, W. Zhang, P. Zhang, W. Ruan, X. Zhu, *J. Agric. Food Chem.* 61 (2013) 41–46.
- [5] C. Hua, Y. Yang, L. Sun, H. Dou, R. Tan, Y. Hou, *Immunobiology* 218 (2013) 292–302.
- [6] W. Jiao, Y. Feng, J.W. Blunt, A.L.J. Cole, M.H.G. Munro, *J. Nat. Prod.* 67 (2004) 1722–1725.
- [7] W. Yan, H.M. Ge, G. Wang, N. Jiang, Y.N. Mei, R. Jiang, S.J. Li, C.J. Chen, R.H. Jiao, Q. Xu, S.W. Ng, R.X. Tan, *Proc. Natl. Acad. Sci. U. S. A.* 111 (2014) 18138–18143.
- [8] C. Chen, J. Wang, J. Liu, H. Zhu, B. Sun, J. Wang, J. Zhang, Z. Luo, G. Yao, Y. Xue, Y. Zhang, *J. Nat. Prod.* 78 (2015) 1193–1201.
- [9] C. Chen, H. Zhu, X.N. Li, J. Yang, J. Wang, G. Li, Y. Li, Q. Tong, G. Yao, Z. Luo, Y. Xue, Y. Zhang, *Org. Lett.* 17 (2015) 644–647.
- [10] CLSI Methods for Determining Bactericidal Activity of Antimicrobial Agents Approved Guideline, document M26-A, Clinical and Laboratory Standards Institute, Wayne, PA, 1999.
- [11] Y. He, Z. Hu, W. Sun, Q. Li, X.N. Li, H. Zhu, J. Huang, J. Liu, J. Wang, Y. Xue, Y. Zhang, *J. Org. Chem.* 6 (2017) 3125–3131.
- [12] Y. He, Z. Hu, Q. Li, X.N. Li, H. Zhu, J. Huang, J. Liu, J. Wang, Y. Xue, Y. Zhang, *J. Nat. Prod.* 80 (2017) 2399–2405.
- [13] Y. Qiao, X. Zhang, Y. He, W. Sun, W. Feng, J. Liu, Z. Hu, Q. Xu, H. Zhu, J. Zhang, Z. Luo, J. Wang, Y. Xue, Y. Zhang, *Sci. Rep.* 8 (2018) 5454–5464.
- [14] C. Chen, Q. Tong, H. Zhu, D. Tan, J. Zhang, Y. Xue, G. Yao, Z. Luo, J. Wang, Y. Wang, Y. Zhang, *Sci. Rep.* 6 (2016) 18711–18718.
- [15] H. Oikawa, Y. Murakami, A. Ichihara, *J. Chem. Soc., Perkin Trans. 1* (1992) 2949–2953.
- [16] S. Sekita, K. Yoshihira, S. Natori, H. Kuwano, *Tetrahedron Lett.* 17 (1976) 1351–1354.
- [17] M. Xue, Q. Zhang, J.M. Gao, H. Li, J.M. Tian, G. Pescitelli, *Chirality* 24 (2012) 668–674.